

Fusion Using Laplacian Pyramid Transform of Light & Dark Channel Priors for Image De-Hazing

Karuna Khatter¹, Bhupender Sharma², Ravi Malik³

¹M.Tech Student Dept. ECE, Geeta Engineering College (Naultha) India

²Assistant Professor Dept. ECE, Geeta Engineering College (Naultha) India

³HOD, ECE Department, Geeta Engineering College (Naultha) India

Abstract-This paper proposes an effective and efficient method for haze removal from a single input image. The method employs both techniques i.e. dark and light channel priors. DCP (Dark channel prior), a scheme for dehazing images represents a statistical property for dehazed single images i.e. most patches for an image contains dark pixels for atleast single color channel. The two main limitations for this method are: 1. For bright image patches, there is over-exposure for atmospheric light, 2. Soft mapping technique applied for dark channel prior to compute factor t (transmission map) costs high. Hence another dehazing algorithm employing both techniques dark and light channel is proposed in this paper where light channel represents a statistics for hazy outdoor images. Furthermore, the guided and bilateral filter are employed for the dark and light channel image refinement. This dehazing algorithm alleviates the above mentioned limitations with Dark channel prior. This paper shows several examples for the comparison for proposed work with the existing Dark channel prior. Further the filters added refine the image to a greater extent. The results comparison prove that this algorithm is 25 times faster than the Dark channel prior. Also the visual quality is much better with the employment of proposed bilateral filter. Therefore the haze effects can be reduced to a great extent and can be utilized for many applications such as intelligent transportation system, aircrafts system, video surveillance, remote sensing etc.

I. INTRODUCTION

Haze is defined as an atmospheric phenomenon in which turbid media obscures the captured scene. Haze causes trouble for almost every computer graphics/vision applications. Effects of haze in the image captured includes reduction in the visibility of the scenes, lowering the reliability of outdoor surveillance systems, reducing the clarity of the satellite images, increasing the color fading, reducing the color contrast of daily photos, creating trouble to the photographers. Hence, haze removal from images is considered as an important and widely challenging topic in computer vision and computer graphics areas. Haze attenuates the light reflected from the scenes causing blending it with some additive light in the atmosphere, resulting in Image degradation as it travels from source to destination. The aim of removing of haze is to get the reflected light from the blended light. To this end, single image haze removal is focused in this thesis. The challenge lies in finding a suitable prior. Priors are important aspects for many algorithms should know for the fact ahead when the fact is not directly known. In general terms, a prior known. In general terms, a prior is defined as statistical/physical properties, rules, or any assumptions. Based on the priori, the algorithms performance is calculated. Several schemes are reported for single image

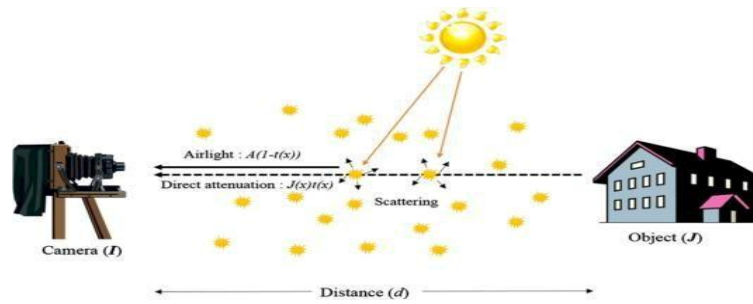


Figure.1: Haze Formation

haze removal. In [9, 13], Rahman suggested singlescale and multi-scale retinex algorithms utilizing the human perception with the Gaussian Blur. The limitation for this algorithm showed floating point calculations, and hence the hazy image developed had a lot of noise, so it was rejected for haze removal. In [11] Narasimhan suggested another novel dehazing algorithm that included unknown depth information along with multiple images required for unknown depth estimation. To remove these limitations, the dehazing algorithms proposed are identified in [2, 6, 15]. The assumptions/ priors in [11, 15] are significantly improved. In [2] Fattal suggested the image albedo and proposed the transmission medium. Again, this approach was not suitable for heavy haze images, thus proving that the assumption is invalid. In [15] Tan revealed that a dehazed image has higher color contrast as compared to the input hazy image and thus proposed for haze removal by maximizing the restored image contrast. However, the proposed Tan's algorithm not only overstretched the color contrast but also introduced the halo artifacts. In [6], another approach for removal of haze was proposed by Dr. He employing Dark Channel Prior, that represents a statistical property for dehazed single images i.e. most patches for an image contains dark pixels for at least single color channel (RGB) excluding the sky and bright area regions. This method resulted in impressive output dehazed image. However this method had two main limitations: 1. For bright image patches, there is over-exposure for atmospheric light, 2. Soft mapping technique applied for dark channel prior to compute factor t (transmission map) costs high. Many more algorithms utilizing Dark channel prior such as mentioned in [8, 10, 12, 14, 16, 17] were proposed. Guided filter in [5][7] is further suggested for image edge-preserving smoothing, that deploys a non-approximate linear time algorithm. This paper proposes an effective and efficient method for haze removal from a single input image. The method employs both techniques i.e. dark and light channel priors. For the local regions, some light pixels represent high intensity for at least single color channel (R,G,B). On the contrary, some dark pixels have very low intensity in at least one color (R,G,B) channel. As per the Dark channel prior theory, the intensity of these dark pixels is devoted due to the airlight component present in input hazy images. But Dr. He utilized the global Atmospheric Light component and not the atmospheric light for every pixel. Hence, the atmospheric light image can further be estimated appropriately by using these light pixels concept. Therefore the two schemes - Dark channel prior and Light channel prior combined, can predict the haze transmission resulting in haze free output image. Further, edge preserving guided filter is used. The image can very well be further refined using a bilateral filter

II. DCP SCHEME AND GUIDED IMAGE FILTERING

The haze imaging equation can be represented as:

$$I(x) = J(x)t(x) + A(1 - t(x)) \quad (1)$$

where $I(x)$ represents input hazy image, $J(x)$ represents output haze free image, A represents global atmospheric light and $t(x)$ represents transmission map. The aim for dehazing is to obtain the refined haze free image $J(x)$ when the input image is $I(x)$. So we need to estimate $t(x)$ and A . The term $J(x)t(x)$ known as

direct attenuation represents scene radiance, while the other term $A(1 - t(x))$ known as airlight represents the scattered light /diffused in air by atmospheric turbids such as dust, haze/ fog etc

A. Dark Channel Prior Scheme

The dark channel prior is a prior that is based on the statistics for outdoor haze-free images. Generally, in most of the local regions that do not cover the sky, it is possible that some dark pixels may have very low intensity in at least one of the color (RGB) channel. The dark channel prior $J(x)$ for any image J is given by [25]:

$$J^{dark}(x) = \min_{x \in \Omega(x)} \left(\min_{c \in (R,G,B)} J^c(x) \right) \quad (2)$$

where J^c represents J color channel and $\Omega(x)$ represents a local patch centered around x . As per dark channel prior for dark regions:

$$J^{dark}(x) \rightarrow 0 \quad (3)$$

Combining the above two equations, transmission \tilde{t} can be estimated as:

$$\tilde{t}(x) = 1 - \min_{x \in \Omega(x)} \left(\min_{c \in (R,G,B)} \frac{I^c(x)}{A^c} \right) \quad (4)$$

The parameter ω is assumed to lie in the range ($0 < \omega < 1$), thus the value for transmission \tilde{t} can be calculated as:

$$\tilde{t}(x) = 1 - \omega * \min_{x \in \Omega(x)} \left(\min_{c \in (R,G,B)} \frac{I^c(x)}{A^c} \right) \quad (5)$$

Further the global atmospheric light A can be computed by picking the brightest pixels with the highest intensity for input image I . The recovered scene radiance can then be further defined as:

$$J(x) = A + \frac{I(x) - A}{\max(t(x), t_0)} \quad (6)$$

where t_0 represents lower bound limit for $t(x)$ with value as 0.1.

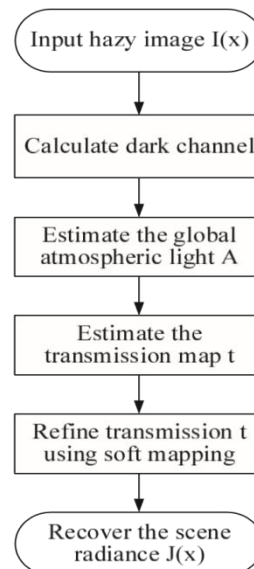


Fig. 1.Flow chart of dark channel prior scheme

The above flowchart depicts the process for Dark Channel Prior scheme. Generally, we can get satisfactory dehazing results by the DCP scheme. The two main limitations for this method are: 1. For bright image patches, there is over-exposure for atmospheric light, 2. Soft mapping technique applied for dark channel prior to compute factor t (transmission map) costs high [18-21].

B. Guided Image Filtering

To refine the transmission t , guided filter is applied. The guided filter represents a local linear model for the guidance I with the filter output q . q represents linear transform of I for window ω_k that is centered around pixel k [25]:

$$q_i = a_k * I_i + b_k \forall i \in \omega_k \quad (7)$$

where the linear coefficients (a_k, b_k) are constant for window ω_k . These linear coefficients (a_k, b_k) can further be set with some value for filter input p . Thus the filter output q needs subtract the unwanted factor n i.e. noise/textures from this filter input p and hence the difference between filter output q and filter input p is to be minimized with the linear model as presented in Equation (7) i.e. the below cost function needs to be minimized in this window ω_k [17].

$$E(a_k, b_k) = \sum \left((a_k * I_i + b_k - p_i)^2 + \epsilon a_k^2 \right) \quad (8)$$

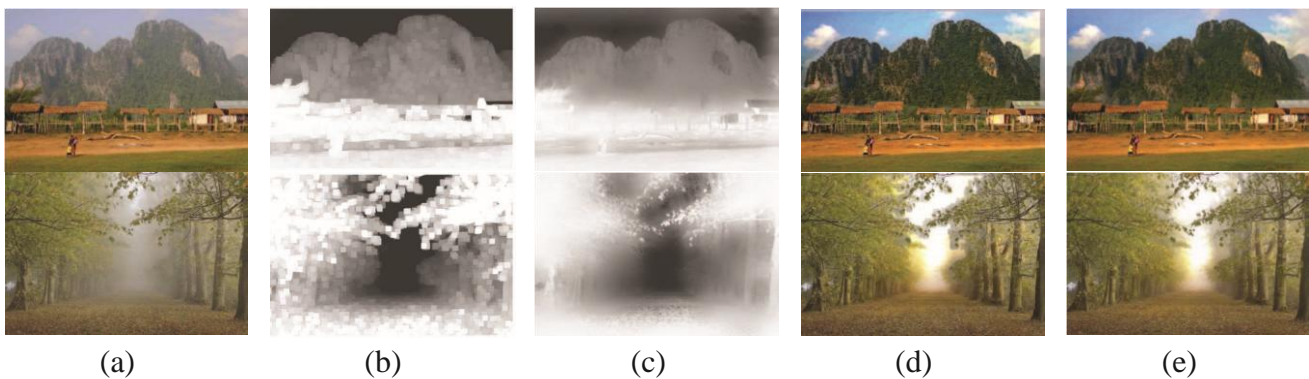


Fig. 2. Haze removal. (a) Input hazy images. (b) Estimated transmission maps before guided filtering. (c) Refined transmission maps after guided filtering.

(d), (e) Recovered images using (b) and (c), respectively.

where ϵ represents regularization parameter for large value of a_k . The solution for Equation (8) are presented in Equation(9), (10):

$$a_k = \frac{\frac{1}{M} \sum_{i \in \omega_k} I_i * p_i - \mu_k * \bar{p}_k}{\sigma_k^2 + \epsilon}$$

$$b_k = \bar{p}_k - a_k * \mu_k$$

where μ_k and σ_k^2 represents mean and variance for the image I in ω_k , M represents the pixel number in ω_k , \bar{p}_k represents the mean value for filter input p in ω_k [13].

$$\bar{p}_k = \frac{1}{M} \sum_{i \in \omega_k} p_i \quad (11)$$

Once the value for the coefficients (a_k, b_k) is obtained for all windows ω_k in the input image I , the filter output q can be calculated as [19]:

$$q_i = \frac{1}{M} \sum_{k|i \in \omega_k} (a_k * I_k + b_k) \quad (12)$$

Further Equation (11) can be reduced to:

$$q_i = \alpha_i * I_i + b_i \quad (13)$$

Advantage of using guided filter is that it enhances the processing speed without altering the filter quality [15].

The below Fig.2b depicts the transmission maps as per Equation(12). On the other hand Fig.2d depicts the corresponding recovered images. Similarly Fig. 2c depicts the refined results with Fig.2b as a constraint. Fig.2e depicts the recovered images as compared to Fig. 2c. Furthermore, the other halo effects and noise are minimized to a much greater extent. The transmission map shows the captured fine image with non-continuous sharp edges, and therefore the object contour is outlined.

III. THE PROPOSED APPROACH

Atmospheric light A considered in almost all the haze removal techniques is the global atmospheric light. Global atmospheric light implies that for every pixel, atmospheric light value is the same. But practically, the atmospheric light for a light pixel cannot be the same as it is for a dark pixel, as shown in below Fig.3:

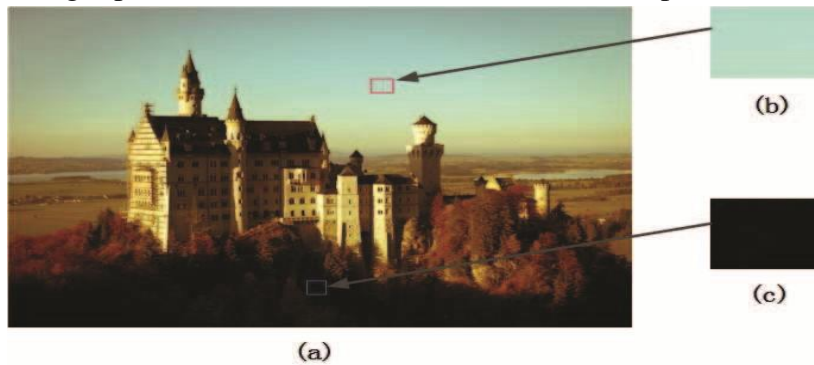


Fig. 3. The contrast of the atmospheric light at different pixel

Its clearly shown in the above fig. that the atmospheric light value for the two pixels as shown in (b) of Fig.3 is not the same as the value for atmospheric light for the pixel in (c). This indicates that the atmospheric light component should be a variable for x where x represents the pixel and can be denoted by $A(x)$. Thus the haze imaging equation Equation (1) can be modified by variable value for atmospheric light i.e. replacing A by $A(x)$ in Equation (1) :-

$$I(x) = J(x)t(x) + A(x)(1 - t(x)) \quad (14)$$

Based on this variable value for atmospheric light, another prior called as light channel prior is advised for image de-hazing. This light channel prior depends on the statistics for outdoor hazy images. Similar to Dark channel prior, light channel prior is based on the fact that almost all patches for the hazy image have some pixels that contain the bright intensities for least one color channel (R, G, B). The light channel $I^{light}(x)$ value for any input image I , can be modelled as [23]:

$$I^{light}(x) = \max_{x \in \Omega(x)} \left(\max_{c \in (R, G, B)} I^c(x) \right) \quad (15)$$

where I^c represents a color channel for the input image I and $\Omega(x)$ represents any local patch centered around any pixel x . For light channel prior, $I^{light}(x)$ i.e. the intensity for light channel should correspond to the atmospheric light component for any haze free image as shown in below equation [24]:

$$J^{light}(x) \rightarrow A^{light}(x) \quad (16)$$

Combining all the above equations for light channel prior, Equation (17) can be derived for atmospheric light component [26]:

$$\tilde{A}(x) = \max_{x \in \Omega(x)} \left(\max_{c \in (R, G, B)} I^c(x) \right) \quad (17)$$

Thus the atmospheric light for a hazy image can be derived by its light channel image component. As the scene radiance value $J(x) \leq A(x)$ for a hazy input image, the atmospheric light component $A(x)$ can be estimated as shown in Equation (18).

$$A(x) = \alpha \tilde{A}(x) + \beta A_0 \quad (18)$$

where A_0 represents the global atmospheric light component, α and β represents the adjustment coefficients with an estimated value $\alpha + \beta < 1.0$.

The below Fig.4 depicts the outdoor hazy images along with the corresponding light channels. These images are first resized with the image width as 600 pixels. Also the dark channel component for these images are calculated with a image patch size for 15×15 .

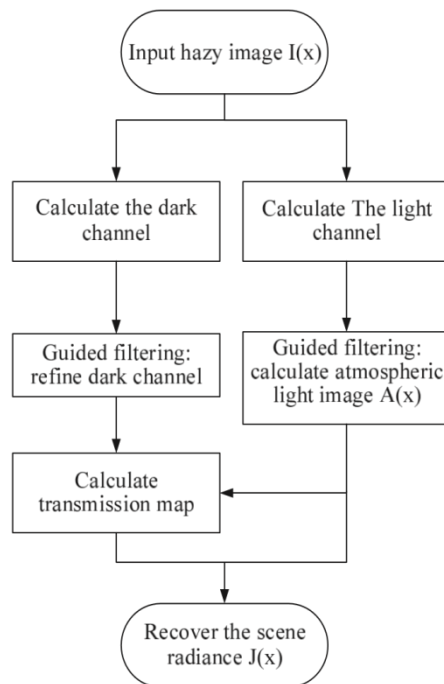


Fig. 5. Flow chart of the proposed scheme

Further the guided filters are applied to refine the images obtained by dark and light channel priors. Let the dark channel refined with this guided filter are denoted by $I^{dark_Guided}(x)$ and let the atmospheric light component after this guided filter is denoted by $A(x)$, the value for transmission map $t(x)$ can be denoted by [26]:

$$t(x) = 1 - \omega * \frac{I^{dark_Guided}(x)}{A(x)} \quad (19)$$

Therefore the recovered de-hazed image is given by Equation (20):

$$J(x) = A(x) + \frac{I(x) - A(x)}{\max(t(x), t_0)} \quad (20)$$

The light channel image as described above can very well be refined in the same fashion as the dark channel image because the output image after the prior contains the halo effects. Thus in order to reduce these halo effects/ noise from the recovered image after the prior, the guided filter is applied for light channel as well.

Fig.5 shows the flow chart for the light channel prior algorithm. The guided filter is applied separately for the two priors i.e. light and dark channel priors and then the value for the transmission map is calculated. Fig.6 shows the refined results for Fig.4b after the guided filter and the two priors are applied to input hazy image. Thus using the guided filter the halo effects/ noise are suppressed, and thus the atmospheric light value is not global and contains different values for different pixels i.e. $A(x)$ [16,18].

IV. EXPERIMENT RESULT

Haze defines the dependency for depth effect when analysing the real-life scenes, thus for simulating this we can divide the image up to 10×10 pixel patches. Here every patch is given a depth gradient ranging in the value 1 to 20. In our experiment, the simulation is done for five images with the same image scene captured at different timings. There is a well-known fact that haze varies with time, hence the simulation is done for different haze values for intensity with assigning all five images, a different values for atmospheric scattering coefficient and the intensity for atmospheric air light. The first one symbolizes the light scattering by haze in scene per unit atmosphere volume. The other one describes the air light intensity that can be seen typically at regions with low horizon considering the real-life image. Further both of these coefficients increase their values corresponding to each other. Scattering coefficients are assigned different values every time along with values of 0.1, 0.15, 0.2, 0.25 and 0.3. This set of values is considered as the most realistic estimates for haze scattering on a scale of 0 to 1. The previous work is referred to get these realistic values.

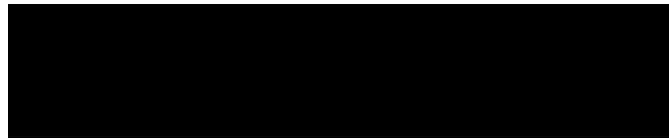


Fig.6: Five images representing increased simulated haze as the scattering increases. The image contains square patches with varying depths (raising from right to left and bottom up). As patches at top are furthest away distance wise they are washed with atmospheric air light.

These images are the comparisons base described in this chapter. These simulations are much accurate as these are based on haze image formation model represented in a dehazing algorithm and described on physics models of radiative transfer for atmosphere. This proves to be effective for the simulation of atmospheric scattering and hence radiance attenuation over distance. As we further investigate these haze images and remember the ground-truth values that are put for these simulations, the accuracy of the algorithms can be tested and hence the algorithms in this research are compared.

The captured image is taken with two polarization values i.e. parallel and perpendicular polarizers and the Fusion procedure is applied for light and dark images pixel values. Further the values for compared images are judged on the basis for different parameters values like L2-color, PSNR_{lum}, PSNR_{split}, Correlation_{lum} and Correlation_{split}. The table below shows the improved values for all these parameters.

Fusion Procedure

The FVID generates the two values for $f_{l_j} N_j = 1$ and the DiffSat maps $f_{DkgMk} = 1$ respectively and fuses both information sources. The LPT fusion process reflect that the different values for DiffSat maps iterating different values in numbers w.r.t. to the regions containing higher fog that further correlate to haze-free processed image iterations. Also, we have various methods for interpolate/ extrapolate the DiffSat set maps to get a new set of various N depth maps figures. Furthermore the new maps are mathematically convolved using a Gaussian kernel function in three dimensions (i.e. x, y, and temporal) that represents a smoothed versions for transitions, which are further normalized to take their sum value with the different set of temporal dimension that involves any pixel x, lets say having value equal to 1. Finally the fused image using LPT (Laplacian Pyramid Transform) is computed to get the correct values.

Consider a dehazed image with name as dehazed2.png, LPT fusion algorithm is applied to this image (this is the same image as taken in base paper 2016 FVID)

Consider the below input image for dehazing (Dehazed2.png)

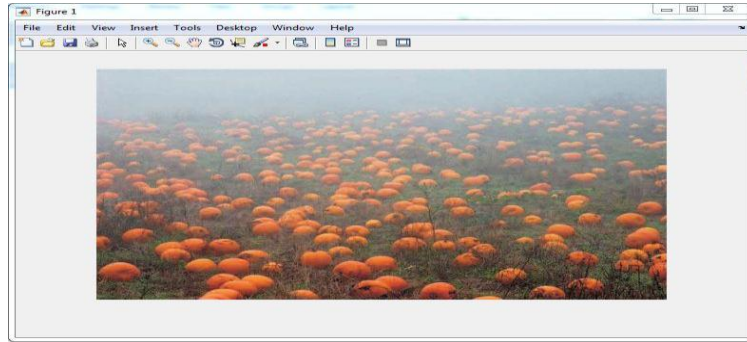


Fig 6. Dehaze Image

The Luminance, saliency and chromatic weight map for the input image (first captured image) is shown below:

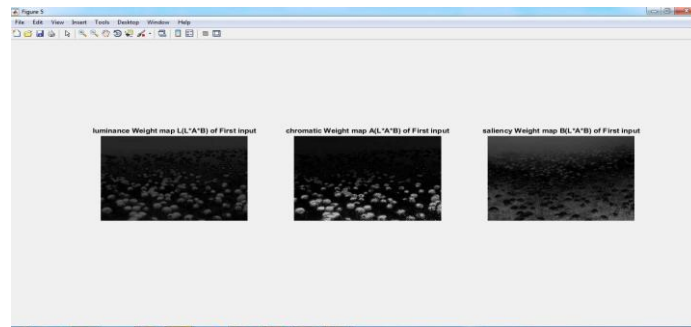


Fig 7. Luminance Measured Image

The Luminance, saliency and chromatic weight map for the input image (second captured image) is shown below:

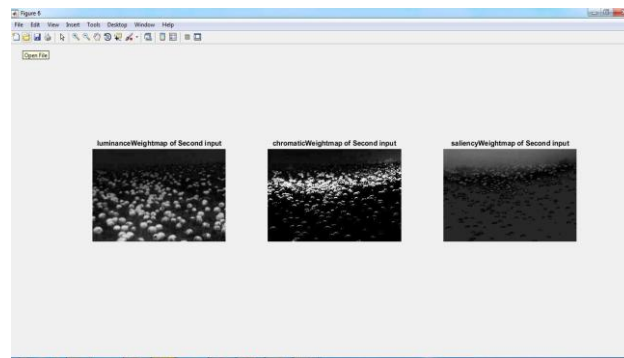


Fig 8. Luminance & Weight Map Measurement

Light and dark channel priors of input image:

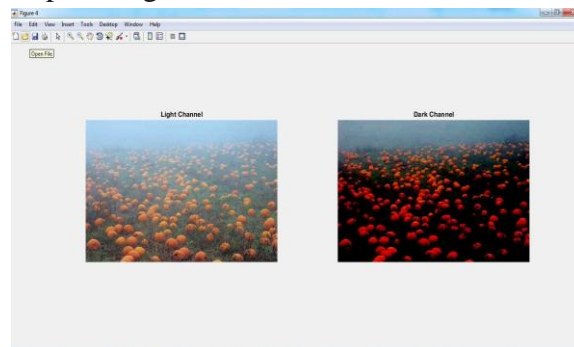


Fig 9. Dark & Light Channel Prior

After histogram Equalization and correcting gamma effects of input captured image:

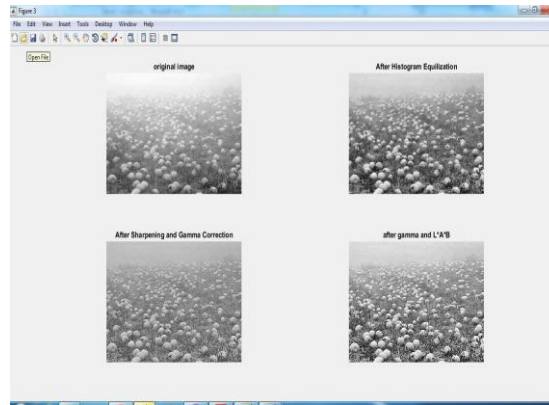


Fig 10. Histogram Equalisation

Final Dehazed image using L^*A^*B enhancement and fusion of Dark and Light channel priors.



Fig 11. Final Dehazed image using L^*A^*B enhancement

The comparison for different parameters like L2-color, PSNRlum, PSNRsplit, Correlationlum, Correlationsplit etc.

QUANTITATIVE RESULTS AS THE MEAN FOR SAMPLEIMAGE (Dehazed2.png)

Error Measure	[28]	[10]	[12]	EVID	FVID	L^*A^*B LVT
L2-color	47.96	52.03	48.93	47.18	44.42	63.474969
PSNRlum	16.03	16.52	15.53	17	17.31	21.001519
PSNRsplit	6.9	6.99	6.79	7.13	7.19	7.935741
Correlationlum	1.24	1.21	1.18	1.25	1.26	2.52216
Correlationsplit	0.7	0.69	0.66	0.71	0.72	0.8417972

V. CONCLUSION

The above described method is Fusion using LPT (Laplacian Pyramid Transform using Dark and Light channel priors). It is significantly extended upon by previously proposed FVID and EVID schemes by gathering information with iterates using different DiffSat maps set coming with extending the algorithms for FVID and EVID image energy. Thus this fusion with visual information appearing from these two techniques determine an effective technique for image dehazing. The proposed technique achieves results in

line with state-of-the-art techniques thereby enhancing far-away regions, while preserving the nearby regions. Hence this appears as an enhancement artifact appearing de-hazing scenes including sky regions. Furthermore, this method flexibility allows to generate various enhancement de-hazing methods enabling other features that will be elaborated in future work.

REFERENCES

1. Kaiming He, Jian Sun, and Xiaoou Tang. Single image haze removal using dark channel prior. *Pattern Analysis and Machine Intelligence, IEEE Transactions on*, 33(12):2341–2353, 2011.
2. Cheng-Hsiung Hsieh, Yu-Sheng Lin, and Chih-Hui Chang. Haze removal without transmission map refinement based on dual dark channels. In *Machine Learning and Cybernetics (ICMLC), 2014 International Conference on*, volume 2, pages 512–516. IEEE, 2014.
3. Daniel J Jobson, Zia-urRahman, and Glenn A Woodell. A multiscale retinex for bridging the gap between color images and the human observation of scenes. *Image Processing, IEEE Transactions on*, 6(7):965–976, 1997.
4. Soo-Chang Pei and Tzu-Yen Lee. Effective image haze removal using dark channel prior and post-processing. In *Circuits and Systems (ISCAS), 2012 IEEE International Symposium on*, pages 2777–2780. IEEE, 2012.
5. Yingchao Song, Haibo Luo, Bing Hui, and Zheng Chang. An improved image de-hazing and enhancing method using dark channel prior. In *Control and Decision Conference (CCDC), 2015 27th Chinese*, pages 5840–5845. IEEE, 2015.
6. Robby T Tan. Visibility in bad weather from a single image. In *Computer Vision and Pattern Recognition, 2008. CVPR 2008. IEEE Conference on*, pages 1–8. IEEE, 2008.
7. Ehsan Ullah, R Nawaz, and Jamshed Iqbal. Single image haze removal using improved dark channel prior. In *Modelling, Identification & Control (ICMIC), 2013 Proceedings of International Conference on*, pages 245–248. IEEE, 2013.
8. Qiang Zhang and Xiaorun Li. Fast image de-hazing using guided filter. In *2015 IEEE 16th International Conference on Communication Technology (ICCT)*, pages 182–185. IEEE, 2015.
9. R. Fattal, “Single Image De-hazing,” in *ACM SIGGRAPH 2008 Papers*, ser. SIGGRAPH ’08. New York, NY, USA: ACM, 2008, pp. 72:1–72:9.
10. J. P. Tarel and N. Hautiere, “Fast visibility restoration from a single color or gray level image,” in *2009 IEEE 12th International Conference on Computer Vision (ICCV)*, Sep. 2009, pp. 2201–2208.
11. K. Nishino, L. Kratz, and S. Lombardi, “Bayesian Defogging,” *International Journal of Computer Vision*, vol. 98, no. 3, pp. 263–278, Jul. 2012.
12. K. He, J. Sun, and X. Tang, “Single Image Haze Removal Using Dark Channel Prior,” *IEEE Transactions on Pattern Analysis and Machine Intelligence*, vol. 33, no. 12, pp. 2341–2353, Dec. 2011.
13. G. Meng, Y. Wang, J. Duan, S. Xiang, and C. Pan, “Efficient Image De-hazing with Boundary Constraint and Contextual Regularization,” in *2013 IEEE International Conference on Computer Vision (ICCV)*, Dec. 2013, pp. 617–624.
14. W. Sun, “A new single-image fog removal algorithm based on physical model” *Optik - International Journal for Light and Electron Optics*, vol. 124, no. 21, pp. 4770–4775, Nov. 2013.
15. Y. Gao, H.-M. Hu, S. Wang, and B. Li, “A fast image de-hazing algorithm based on negative correction,” *Signal Processing*, vol. 103, pp. 380–398, Oct. 2014.
16. J.-B. Wang, N. He, L.-L. Zhang, and K. Lu, “Single image de-hazing with a physical model and dark channel prior,” *Neurocomputing*, vol. 149, Part B, pp. 718–728, Feb. 2015.

17. Q. Zhu, J. Mai, and L. Shao, "A Fast Single Image Haze Removal Algorithm Using Color Attenuation Prior," *IEEE Transactions on Image Processing*, vol. 24, no. 11, pp. 3522–3533, Nov. 2015.
18. Z. Li and J. Zheng, "Edge-Preserving Decomposition-Based Single Image Haze Removal," *IEEE Transactions on Image Processing*, vol. 24, no. 12, pp. 5432–5441, Dec. 2015.
19. Y.-H. Lai, Y.-L. Chen, C.-J. Chiou, and C.-T. Hsu, "Single-Image Dehazing via Optimal Transmission Map Under Scene Priors," *IEEE Transactions on Circuits and Systems for Video Technology*, vol. 25, no. 1, pp. 1–14, Jan. 2015.
20. K. Tang, J. Yang, and J. Wang, "Investigating Haze-Relevant Features in a Learning Framework for Image Dehazing," in *2014 IEEE Conference on Computer Vision and Pattern Recognition (CVPR)*, Jun. 2014, pp. 2995–3002.
21. B. Cai, X. Xu, K. Jia, C. Qing, and D. Tao, "DehazeNet: An End-to-End System for Single Image Haze Removal," *IEEE Transactions on Image Processing*, vol. 25, no. 11, pp. 5187–5198, Nov. 2016.
22. L. K. Choi, J. You, and A. C. Bovik, "Referenceless Prediction of Perceptual Fog Density and Perceptual Image Defogging," *IEEE Transactions on Image Processing*, vol. 24, no. 11, pp. 3888–3901, Nov. 2015.
23. R. Tan, "Visibility in bad weather from a single image," in *2008 IEEE Conference on Computer Vision and Pattern Recognition (CVPR)*, Jun. 2008, pp. 1–8.
24. J. Oakley and H. Bu, "Correction of Simple Contrast Loss in Color Images," *IEEE Transactions on Image Processing*, vol. 16, no. 2, pp. 511–522, Feb. 2007.
25. C. Ancuti and C. Ancuti, "Single Image Dehazing by Multi-Scale Fusion," *IEEE Transactions on Image Processing*, vol. 22, no. 8, pp. 3271–3282, Aug. 2013.
26. V. De Dravo and J. Hardeberg, "Stress for dehazing," in *Colour and Visual Computing Symposium (CVCS)*, 2015, Aug. 2015, pp. 1–6.
27. K. Gibson and T. Nguyen, "Fast single image fog removal using the adaptive Wiener filter," in *2013 20th IEEE International Conference on Image Processing (ICIP)*, Sep. 2013, pp. 714–718.